Oceanic excitations on polar motion: a cross comparison among models

Y. H. Zhou,[1,4] J. L. Chen,[2] X. H. Liao[1,4] and C. R. Wilson[2,3]

[1]*Shanghai Astronomical Observatory, Chinese Academy of Sciences, 80 Nandan Road, Shanghai 200030, China. E-mail: yhzhou@shao.ac.cn*
[2]*Center for Space Research, University of Texas at Austin, Austin, TX 78712, USA*
[3]*Department of Geological Sciences, University of Texas at Austin, Austin, TX 78712, USA*
[4]*United Center for Astrogeodynamical Research, Chinese Academy of Sciences, Shanghai, China*

SUMMARY

Recent studies based on various ocean general circulation models (OGCMs) demonstrate that the oceans are a major contributor to polar motion excitations. In this paper, we analyse and compare observed non-atmospheric polar motion excitations with oceanic angular momentum (OAM) variations determined from four OGCMs, which include the parallel ocean climate model (POCM), a barotropic ocean model (BOM), the Estimating the Circulation and Climate of the Ocean (ECCO) non-data-assimilating model (ECCO-NDA) and the ECCO data-assimilating model (ECCO-DA). The data to be analysed span a 5-yr overlapped period from 1993 to 1997. At annual timescale, considerable discrepancies exist between POCM and the other three models, which result mainly from differences in annual components of the forcing wind fields. At semi-annual timescale, however, POCM shows better phase agreement with observed non-atmospheric polar motion excitation than the other three ocean models. At intraseasonal timescales, ECCO-DA yields better agreement with observations, and reduces the variance of non-atmospheric excitations by ∼60 per cent, 10–20 per cent more than those explained by the other three models. However, at the very short periods of 4–20 days, the BOM estimates could explain about half of the observed variance, twice as much as that by ECCO-NDA, and also shows considerably better correlation with observations. Due to different modelling schemes and methods, significant discrepancies could arise with respect to the quality of modelling large-scale oceanic mass redistribution and current variation. A complete understanding of global oceanic contributions to polar motion excitation still remains a challenge.

Key words: excitation, ocean general circulation model (OGCM), oceanic angular momentum (OAM), polar motion.

1 INTRODUCTION

The motion of the Earth's instantaneous rotation pole within the terrestrial reference frame is briefly referred to as the Earth's polar motion (Lambeck 1980). Polar motion includes a linear trend (secular part), periodic changes of 12 months and 14 months, that is, the annual and Chandler wobbles, and quasi-periodic variations on intraseasonal, interannual and decadal time scales (e.g. Eubanks 1993; Zhou *et al.* 1998; Natsula *et al.* 2002). On timescales from a few days to a few years, polar motion is primarily driven by air and water mass redistribution and movement within the Earth system. Atmospheric winds and surface pressure changes are found to excite a significant portion of observed polar motion (e.g. Chao & Au 1991). Water mass redistribution within the oceans and continental water storage change are also believed to play major roles (e.g. Wahr 1983; Chen *et al.* 2000). Recent studies based on the parallel ocean

climate model (POCM), the Estimating the Circulation and Climate of the Ocean (ECCO) non-data-assimilating model (ECCO-NDA), the ECCO data-assimilating model (ECCO-DA) and a barotropic ocean model (BOM) demonstrate that oceanic mass redistribution and circulation provide important contributions to the excitation of polar motion that has not been accounted for by the atmosphere, on seasonal, intraseasonal and interannual timescales (Ponte *et al.* 1998, 2001; Johnson *et al.* 1999; Ponte & Stammer 1999; Ponte & Ali 2002; Gross *et al.* 2003b; Chen *et al.* 2004).

Because of different modelling schemes and methods, discrepancies could arise with respect to the quality of modelling large-scale oceanic mass redistribution and current variation, which in turn affects the quantitative assessment of oceanic effects on the Earth's polar motion. So far, quantitative assessment of the differences in estimating oceanic contributions to the polar motion among different ocean general circulation models (OGCMs) remains unclear. In

the following section, we compute geodetic polar motion excitation function by de-convolving observed polar motion series, using a state-of-the-art two-stage filter that produces better amplitude accuracy at high frequencies than traditionally used one-stage filter (Wilson & Chen 1996). Non-atmospheric polar motion excitation function is subsequently obtained by removing atmospheric angular momentum (AAM) contributions from observed polar motion excitations. In Section 3, we introduce oceanic angular momentum (OAM) function determined from four OGCMs, that is, POCM, BOM, ECCO-NDA and ECCO-DA. The four OAM functions and observed non-atmospheric polar motion excitation, within a 5-yr overlapped period from 1993 to 1997, are compared and analysed in Section 4. Finally, we summarize the results in Section 5.

2 NON-ATMOSPHERIC POLAR MOTION EXCITATIONS

2.1 'Observed' polar motion excitations

In terrestrial coordinate system, polar motion is usually expressed as a complex function $m(t) = m_x(t) + im_y(t)$, where $m_x(t)$ and $m_y(t)$ are components along the Greenwich Meridian and the $90°$E longitude, respectively. The excitation of polar motion is depicted as (Lambeck 1980):

$$m(t) + (i/\sigma_c)\dot{m}(t) = \psi(t), \tag{1a}$$

where $\psi(t) = \psi_x(t) + i\psi_y(t)$ with $\psi_x(t)$ and $\psi_y(t)$ being the x and y components, respectively, of geodetic or 'observed' polar motion excitation function, $\sigma_c = 2\pi F_c(1 + i/2Q)$ is the complex Chandler frequency, F_c is about 0.843 cycles yr^{-1}, and Q is the damping factor. The transfer function of this equation, which is the ratio of the Fourier transform of $m(t)$ to that of $\psi(t)$ at frequency f, is

$$L_1(f) = \frac{\sigma_c}{\sigma_c - 2\pi f}. \tag{1b}$$

The discrete version of eq. (1) was developed by Wilson (1985),

$$\psi(t) = \frac{i\exp(-i\pi F_c T)}{\sigma_c T}[m(t + T/2) - \exp(i\sigma_c T)m(t - T/2)], \tag{2a}$$

where T is the sampling interval. The corresponding transfer function is

$$L_2(f) = \frac{-i\sigma_c T \exp[i\pi(F_c - f)T]}{1 - \exp[i(\sigma_c - 2\pi f)T]}. \tag{2b}$$

The curve labelled (2b/1b) in Fig. 1 shows the error in the application of eq. (2a) relative to the exact result eq. (1a) for the case $T = 1$ day, $F_c = 0.843$ cycles per year and $Q = 179$. The amplitude difference is given by the ratio of amplitude response (2b)/(1b) minus 1. Obviously, the phase response of eq. (2b) almost perfectly duplicates the desired response of (1b), while the amplitude response deviates at high frequencies. For example, at the frequency of 0.3 cycles per day (in this example), the error of amplitude response could reach as much as ~20 per cent.

Wilson & Chen (1996) further designed a digital filter, which corrects the amplitude response error of (2a), but does not alter the phase. The zero-phase requirement is easily implemented by passing it over the data in both forward and reverse directions. The two-stage filter and its transfer function are

$$\psi^1(t) = k_1 \exp(i\sigma_c T)\psi(t) + k_2 \exp(i2\sigma_c T)\psi(t - T)$$
$$+ k_3 \exp(i\sigma_c T)\psi^1(t - T) + k_4 \exp(i2\sigma_c T)\psi^1(t - 2T) \tag{3a}$$

and

$$L_3(f) =$$
$$\frac{c_1 \exp(-i\sigma_c T) + c_2 \exp(-i2\pi fT) + c_3 \exp[i(\sigma_c - 4\pi f)T]}{1 - c_4 \exp[i(\sigma_c - 2\pi f)T]}, \tag{3b}$$

where $c_1 = 0.9304$; $c_2 = 0.5024$; $c_3 = 0.01861$; $c_4 = -0.4541$; $k_1 = 1/c_1 = 1.0748$; $k_2 = -c_4/c_1 = 0.4881$; $k_3 = -c_2/c_1 = -0.5400$; and $k_4 = -c_3/c_1 = -0.0200$. The superscript designation, $\psi^1(t)$, indicates the excitation time-series after the first (forward direction) application to the output of filter (2a). Note that the eq. (3a) is a corrected version of eq. (4a) in Wilson & Chen (1996), in which $\psi^1(t)$ is mistakenly typed as $\psi(t)$ and vice versa. The filter is then applied a second time in the reverse direction. The final response is $|L_3(f)|^2$.

The curve labelled (3b/1b) in Fig. 1 displays the error associated with the application of eq. (2a) followed by eq. (3a). The two-stage filter method produces much better amplitude accuracy at the very high frequencies than previous generally used one-stage filter. Therefore, this approach should be applied when dealing with high-frequency polar motion variation, for instance, at frequencies above 0.1 cycles per day for 1-day interval data.

Observed polar motion time-series are from SPACE2002 (Gross 2003a), provided by the Jet Propulsion Laboratory (JPL). Daily SPACE2002 EOP time series are sampled at midnight and cover the period from 1976 to 2002. They are obtained through a Kalman filter combination of the Earth orientation measurements from advanced space-geodetic techniques including the lunar and satellite laser ranging, very long baseline interferometry, and the global positioning system. Observed polar motion excitations are computed using the above two-stage filter method (eqs 2a and 3a), with $F_c = 0.843$ cycles per year and $Q = 179$ (Wilson & Vicente 1990).

2.2 Atmospheric angular momentum excitations

Polar motion is excited by mass motion (e.g. winds and currents) and surface mass load (e.g. atmospheric pressure and oceanic bottom pressure) variations. The 'geophysical' polar motion excitation, $\chi(t) = \chi_x(t) + i\chi_y(t)$, is a function of changes in relative angular momentum, $h(t) = h_x(t) + ih_y(t)$, and of changes in the Earth's inertia tensor, $c(t) = \Delta I_{xz}(t) + i\Delta I_{yz}(t)$ (Gross *et al.* 2003b):

$$\chi(t) = [1.61h(t) + 1.12\Omega c(t)]/[\Omega(C - A)], \tag{4}$$

where $(\chi_x(t), \chi_y(t))$, $(h_x(t), h_y(t))$ and $(\Delta I_{xz}(t), \Delta I_{yz}(t))$ are the x and y components, respectively of $\chi(t)$, $h(t)$ and $c(t)$. Ω is the Earth's mean angular velocity, C and A are the polar and equatorial moments of the inertia of the entire Earth. The factor of 1.61 accounts for effects of rotational deformation and core decoupling, and the factor of 1.12 includes the above two effects as well as the surface loading effect on the solid Earth (Wahr 1982; Gross *et al.* 2003b).

AAM time-series are provided by the International Earth Rotation Service (IERS) Special Bureau for the Atmosphere (SBA) (Salstein *et al.* 1993), and are computed using wind velocity and surface air pressure data derived from the National Centers for Environmental Prediction/National Center for Atmospheric Research (NCEP/NCAR) reanalysis project (Kalnay *et al.* 1996). The angular momentum carried by the winds (the 'wind' term) is integrated from 1000 hpa at the surface to top of the model at 10 hpa, and the angular momentum due to surface pressure variations (the 'pressure' term) is computed based on the inverted barometer (IB) assumption (Salstein *et al.* 1993). The IB assumes that the ocean responds to the atmospheric loading isostatically. In order to match the temporal
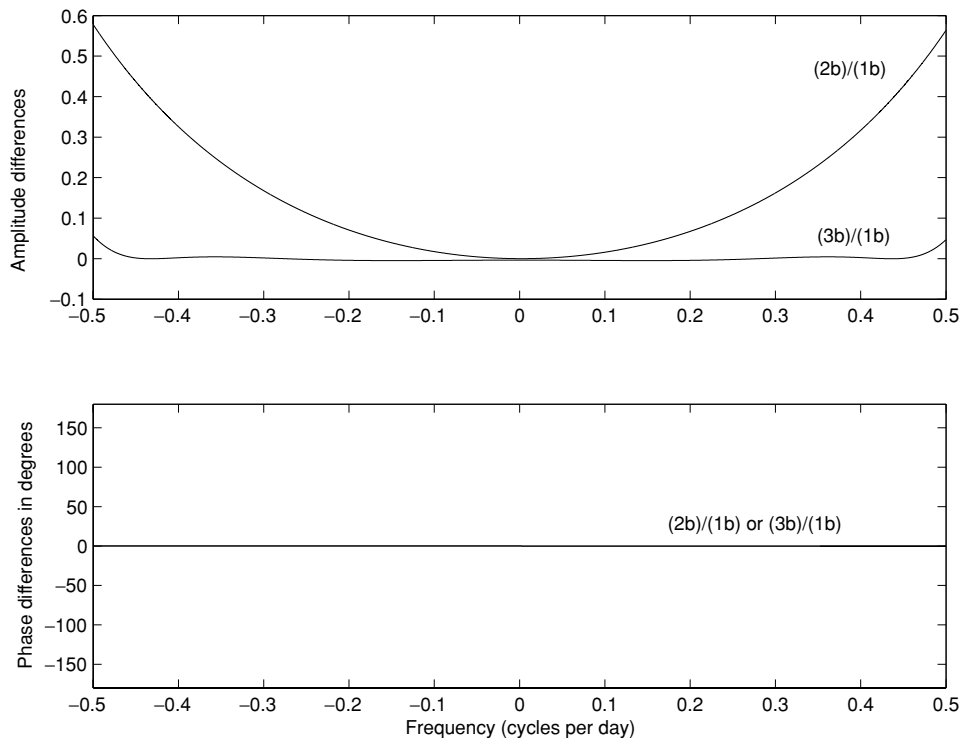
Figure 1. Errors in amplitude and phase of the transfer function for digital filter methods. Curves labelled (2b/1b) gives the error in the application of eq. (2a) relative to the exact result eq. (1a). Curves labelled (3b/1b) gives the error associated with the application of eq. (2a) followed by eq. (3a). The amplitude difference is given by the ratio of amplitude response minus 1. The two-stage filter method produces better amplitude accuracy at high frequencies.

resolution of the 'observed' polar motion excitations, the 6-hourly NCEP/NCAR reanalysis AAM results are averaged daily by summing five consecutive values using weights of 1/8, 1/4, 1/4, 1/4, and 1/8. Non-atmospheric polar motion excitations are readily acquired using the differences between 'observed' and atmospheric polar motion excitations.

3 OCEANIC ANGULAR MOMENTUM EXCITATIONS

The OAM excitations can be computed using velocities of ocean currents, sea level, temperature, salinity and ocean bottom pressure, estimated from OGCMs. The OAM excitations include two types of contributions, that is, the angular momentum change carried by ocean currents and the angular momentum change due to ocean bottom pressure (OBP) variations. In this study, we employ the OAM results determined from four OGCMs: the POCM, BOM, ECCO-NDA and ECCO-DA. The POCM (Stammer *et al.* 1996; Johnson *et al.* 1999), BOM (Ponte 1993; Ponte & Ali 2002) and ECCO-NDA (Gross *et al.* 2003b) OAM results are provided by the IERS Special Bureau for the Oceans (at http://euler.jpl.nasa.gov/sbo/). The ECCO-DA OAM results are the same as published by Chen *et al.* (2004).

POCM is a free-surface, wind-stress and heat-flux driven OGCM that is based on the primitive equations under the hydrostatic and Boussinesq approximations (Stammer *et al.* 1996; Johnson *et al.* 1999). It is forced by surface wind stresses and surface heat fluxes derived from the European Centre for Medium-Range Weather Forecasts (ECMWF). The model covers the global ocean from 75°S to 65°N with a horizontal resolution of 0.4°in longitude and average

0.25° in latitude and a vertical resolution of 20 layers. The model employs realistic coastlines and bathymetry. Data products are available every 3 days from 1988 to 1997.

BOM is a constant-density, shallow-water numerical model driven by NCEP/NCAR surface wind and barometric pressure fields (Ponte 1993; Ponte & Ali 2002). The configuration of the model has been optimized to explain sea level variance in the TOPEX/Poseidon altimeter data. The model includes an improved representation of topography and realistic coastlines. Simulated OAM time-series at daily intervals during the period of 1992 October to 2000 June are from Ponte & Ali (2002).

ECCO-NDA is based on the Massachusetts Institute of Technology general circulation model (Marshall *et al.* 1997a,b; Gross *et al.* 2003b). The model is forced by surface wind stresses and surface heat fluxes and evaporation–precipitation fields from the NCEP/NCAR reanalysis project. It spans 73.5°S to 73.5°N latitude with a latitudinal spacing ranging between 1/3° at the equator to 1° at the poles and a longitudinal grid spacing of 1°. The model has 46 levels ranging in thickness from 10 m at the surface to 400 m at depth. The model employs realistic boundaries and bottom topography. The resulting modelled OAM span 1980 January to 2003 March at daily intervals. The ECCO-DA is virtually the same model as ECCO-NDA, but assimilates TOPEX/Poseidon sea surface height observations and covers the periods from 1993 to the present (Chen *et al.* 2004). The durations and sampling intervals of non-atmospheric polar motion excitations (SPACE2002-AAM) and OAM excitations determined from the four OGCMs are summarized in Table 1. For clarity, the individual contributions from OBP variations and ocean currents will be referred to hereafter as that due to 'OBP' and 'Currents', respectively.

Table 1. Summary of durations and sampling intervals of polar motion excitation functions from observations (SPACE2002-AAM) and four oceanic general circulation models (OGCMs). (A) OBP terms; (B) Currents terms.

Excitation function	Duration	Sampling interval (days)
SPACE2002-AAM	1976.09–2003.01	1
(A) OBP		
POCM	1988.01–1997.12	3
BOM	1992.10–2000.06	1
ECCO-NDA	1980.01–2002.03	1
ECCO-DA	1993.01–2003.12	0.5
(B) Currents		
POCM	1988.01–1997.12	3
BOM	1992.10–2000.06	1
ECCO-NDA	1980.01–2002.03	1
ECCO-DA	1993.01–2003.12	10

OBP: ocean bottom pressure; SPACE2002-AAM: observed non-atmospheric excitation; POCM: the parallel ocean climate model; BOM: a barotropic ocean model; ECCO-NDA: the Estimating the Circulation and Climate of the Ocean (ECCO) non-data-assimilating model; ECCO-DA: the ECCO data-assimilating model.

4 COMPARISON AND RESULT

The data to be analysed span a 5-yr overlapped period from 1993 to 1997. In the studies of seasonal and intraseasonal variations, non-atmospheric polar motion excitations and four OAM contributions are all re-sampled into 10-day intervals, to match the temporal resolution of ECCO-DA OAM currents term (Sections 4.1 and 4.2). In the studies of high-frequency variations of 4–20 days daily BOM and ECCO-NDA OAM contributions are compared with non-atmospheric polar motion excitations. The POCM and ECCO-DA OAM results are not employed in the high-frequency study because their larger sampling intervals will hinder analyses on the high-frequency band.

4.1 Seasonal variations

A linear combination of a trend, annual, semi-annual and terannual terms is fitted to non-atmospheric polar motion excitations and four

Table 2. Amplitude and phase of the prograde and retrograde components of annual polar motion excitation functions from observations (SPACE2002-AAM) and four OGCMs. The reference date for phase is 1990 January 1, 0000UT. (A) OBP terms; (B) Currents terms; (C) OBP plus Currents terms.

	Annual prograde		Annual retrograde	
Excitation function	Ampli., mas	Phase, deg	Ampli., mas	Phase, deg
SPACE2002-AAM	8.53	38.3	9.11	106.0
(A) OBP				
POCM	5.99	133.6	4.08	10.8
BOM	2.53	37.7	2.41	113.2
ECCO-NDA	3.04	65.8	3.15	112.9
ECCO-DA	3.84	73.5	1.92	101.2
(B) Currents				
POCM	1.65	49.8	3.29	26.4
BOM	2.10	24.0	1.85	93.5
ECCO-NDA	2.10	50.3	2.16	47.0
ECCO-DA	2.77	25.5	2.09	24.0
(C) OBP+Currents				
POCM	6.39	118.7	7.30	17.8
BOM	4.60	31.5	4.20	104.7
ECCO-NDA	5.10	59.5	4.49	86.8
ECCO-DA	6.06	53.6	3.14	60.6

OAM contributions in a least squares sense. Table 2 shows the results of this fit for the amplitude A and phase α of the prograde (subscript p) and retrograde (subscript r) components of the excitation of annual polar motion defined by (Munk & MacDonald 1960)

$$\chi(t) = A_p e^{i\alpha_p} e^{i\sigma(t-t_0)} + A_r e^{i\alpha_r} e^{-i\sigma(t-t_0)}, \qquad (5)$$

where σ is the annual frequency and the reference date t_0 is 1 January 1990, 0000UT.

Fig. 2 shows the phasor diagram of the prograde (top) and retrograde (bottom) components of annual wobble excitation functions from observations (SPACE2002-AAM) and four OGCMs. It is seen that relatively large discrepancies exist between POCM and the other
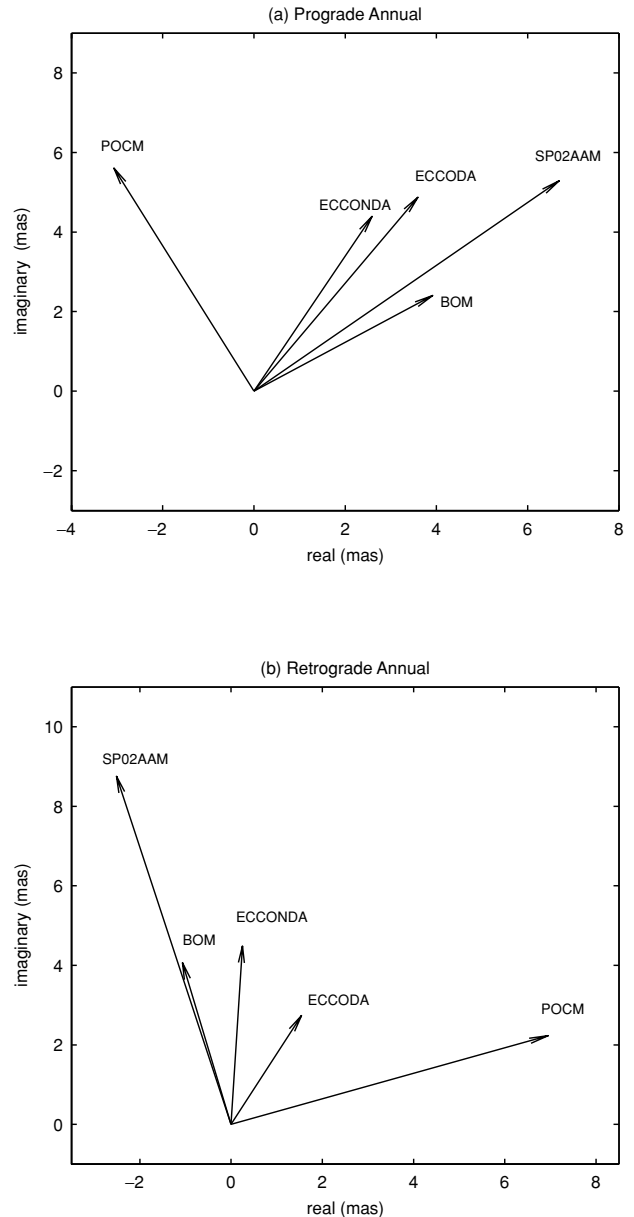

Figure 2. Phasor diagrams of the prograde and retrograde components of annual polar motion excitation functions (as of January 1) from observations (SPACE2002-AAM) and four oceanic general circulation models (OGCMs). POCM: the parallel ocean climate model; BOM: an barotropic ocean model; ECCO-NDA: the Estimating the Circulation and Climate of the Ocean (ECCO) non-data-assimilating model; ECCO-DA: the ECCO data-assimilating model.
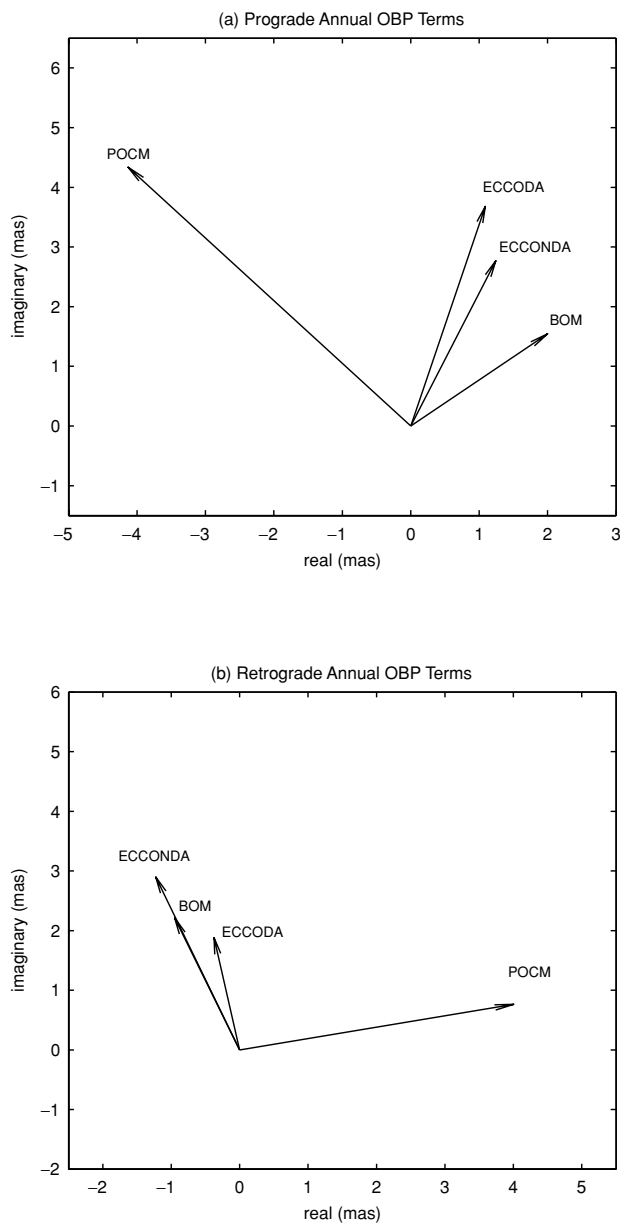
Figure 3. As in Fig. 2 but for the OBP terms of the annual polar motion excitations.

Figure 4. As in Fig. 2 but for the currents terms of the annual polar motion excitations.

three models either for the prograde components or for the retrograde components. Figs 3 and 4 separately exhibit the OBP terms and currents terms of OAM excitations at annual timescale. Obviously, the discrepancy between POCM and the other three OGCMs comes predominantly from the disparity in the OBP terms. The systematic discrepancy is mainly due to the difference in the forcing wind fields. The POCM model is driven by the ECMWF operational wind field while the other models are driven by surface wind fields derived from the NCEP reanalysis project. An examination of the AAM produced from NCEP Reanalysis and ECMWF operational models has shown differences between these models at annual period. The OAM estimates produced by different ocean models are directly affected by the atmospheric models used to force the ocean model (Johnson 2005).

Tables 3 lists corresponding results for the excitation of semi-annual and terannual polar motion. Fig. 5 shows the phasor diagram
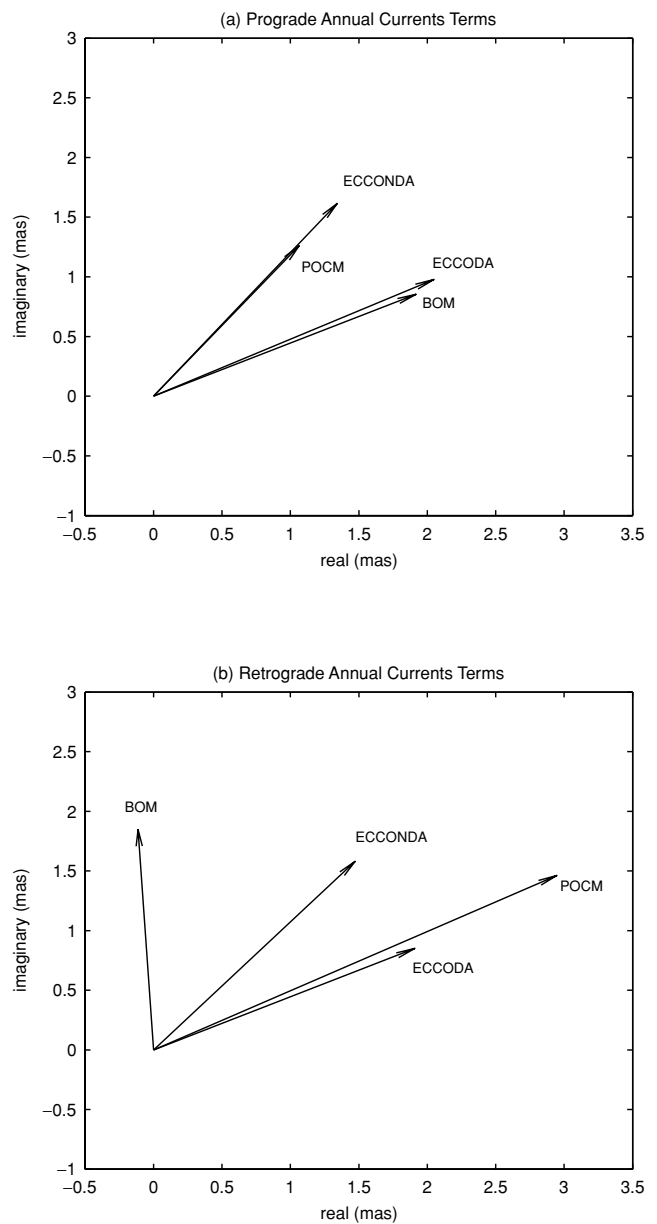
of the prograde and retrograde components of the semi-annual wobble excitation functions from observations (SPACE2002-AAM) and four OGCMs. The four models agree quite well in phase at the prograde semi-annual period. For either prograde or retrograde components, the POCM result shows better agreement in phase with observed non-atmospheric polar motion excitation than the other three ocean models.

Fig. 6 displays the phasor diagram of the prograde and retrograde components of the terannual wobble excitation functions from observations (SPACE2002-AAM) and four OGCMs. In view of Figs 2–6, considerable discrepancies remain between observed non-atmospheric polar motion excitations and the four OAM contributions at annual, semi-annual and terannual frequencies. This may reflect errors in observed and/or modelled excitations, but may also imply that other unaccounted sources, like continental water storage change, may have important effects on seasonal polar motion

Table 3. As in Table 2 but for the semi-annual and terannual polar motion excitations.

Excitation function	Semi-annual prograde		Semi-annual retrograde		Terannual prograde		Terannual retrograde	
	Ampli., mas	Phase, deg	Ampli., mas	Phase, deg	Ampli., mas	Phase, deg	Ampli., mas	Phase, deg
SPACE2002-AAM	5.98	163.7	2.29	−148.6	3.93	35.8	1.80	−85.0
(A) OBP								
POCM	1.33	155.7	2.27	−153.1	1.06	68.5	1.35	−2.9
BOM	1.31	156.8	1.60	−127.5	0.89	100.2	0.86	−82.8
ECCO-NDA	1.01	167.6	2.17	−134.9	1.10	94.6	1.04	−62.8
ECCO-DA	1.86	−179.1	2.17	−123.4	1.06	31.0	0.77	−102.1
(B) Currents								
POCM	1.04	176.3	1.12	−165.7	1.20	65.6	1.26	−37.7
BOM	1.23	175.5	1.38	−109.9	1.18	62.5	0.76	−7.4
ECCO-NDA	1.45	170.9	1.69	−132.0	0.89	78.7	0.79	−32.4
ECCO-DA	2.14	171.8	1.48	−96.7	0.85	66.7	0.10	−153.2
(C) OBP+Currents								
POCM	2.33	164.7	3.38	−157.3	2.26	66.9	2.49	−19.6
BOM	2.50	165.9	2.95	−119.3	1.96	78.6	1.28	−48.0
ECCO-NDA	2.45	169.6	3.86	−133.6	1.97	87.5	1.78	−49.7
ECCO-DA	3.99	176.0	3.56	−112.6	1.82	46.7	0.84	−107.5

(e.g. Chao & O'Connor 1988; Kuehne & Wilson 1991; Chen *et al.* 2000; Gross *et al.* 2003b). This subject is beyond the scope of the presented study and awaits further investigations.

4.2 Intraseasonal variation

We first remove from each excitation a linear combination of a trend, annual, semi-annual and terannual terms that was fitted by the least-squares method (see Section 4.1). Then, the residual series is passed through a Butterworth high-pass filter of order 2, in both forward and reverse directions to eliminate any phase distortion (Wiley 1979). The cut-off frequency is 1 cycle per year (cpy). Thus the resulted series is considered as the intraseasonal variation used in the following cross correlation and variance analyses.

The cross correlation coefficients between intraseasonal non-atmospheric polar motion excitations and OAM excitations from the four OGCMs, and the percentage of observed non-atmospheric excitation explained by each modelled oceanic contribution are assembled in Table 4. X gives the results for the x component, Y for the y component, and $X + iY$ for the complex-values $X + iY$ component. All four OGCMs demonstrate that the OBP term has generally stronger correlation with the observed and accounts for more observed excitation variance than the current term, that is the OBP term contributes more to observed non-atmospheric excitation than ocean current term. Combined excitations from both OBP and current terms can explain more observed excitation than either one alone.

By the comparing the four OGCM estimates, we further notice that the ECCO-DA estimate yields the best agreement with observations among the four OGCMs. This model shows the strongest correlation (as high as 0.79) with non-atmospheric polar motion excitations and reduces the variance of non-atmospheric excitations by 60.9 per cent, about 10–20 per cent more than those explained by the other three models. This may, from an independent point of view, substantiate that the ECCO ocean model, after assimilating the TOPEX/Poseidon sea surface height observations, produces relatively good simulation of oceanic variations within the intraseasonal frequency band (Stammer *et al.* 2002).

4.3 High frequency variations of 4–20 day

Fig. 7 shows multitaper squared coherences (A1, A2) and phases (B1, B2) of SPACE2002-AAM with oceanic excitations modelled

from BOM and ECCO-NDA within the high-frequency band. The trend, annual, semi-annual and terannual variations have been removed from all time-series by least-squares fitting. The multitaper technique of Thomson (1982) is applied in computing the spectra; it provides robust, minimum-leakage spectral estimates. Seven orthogonal tapers with time-bandwidth of 4π were adopted. The horizontal dash lines in A1 and A2 indicate 95 per cent confidence threshold for the squared coherence. It is obvious that the BOM estimates exhibit stronger coherence with SPACE2002-AAM than the ECCO-NDA estimates. The squared coherence between BOM and SPACE2002-AAM exceeds 95 per cent threshold at a broader high-frequency band than that between ECCO-NDA and SPACE2002-AAM. Meanwhile, the coherence phase between BOM and SPACE2002-AAM has smaller variation amplitude around the zero-degree phase line than that between ECCO-NDA and SPACE2002-AAM.

We further focus our study within a high-frequency band of 4–20 days. The high-frequency variation of 4–20 days is extracted by removing from each excitation time-series a trend and seasonal terms and by passing the residual series through a Butterworth bandpass filter of order two with cut-off frequencies of 1/4 and 1/20 cycles per day. The correlation study and variance analysis result between non-atmospheric polar motion excitation and oceanic effects modelled from BOM and ECCO-NDA is listed in Table 5. Similar to the results in intraseasonal band, for both BOM and ECCO-NDA, the OBP term explains more observed non-atmospheric excitation than the current term. Combined OBP and current excitations can account for more observed excitation than either one alone.

By comparing the BOM and ECCO-NDA simulation results, it is easily seen that the BOM estimates could explain about half of the observed variance, over twice as much as that by ECCO-NDA (51.6 per cent vs. 24.8 per cent), and also shows considerably better correlation with observations (0.73 vs. 0.54). This is consistent with the frequency-domain coherence result shown in Fig. 7. The superiority of BOM estimates to those from ECCO-NDA in modelling high frequency OAM variation may result from two factors:

(1) BOM is forced by the surface wind field as well as barometric pressure, while the atmospheric pressure is not included in the ECCO_NDA model's forcing fields. This result demonstrates the importance of including pressure-forcing effects when modelling the high-frequency variability of the ocean (Ponte & Ali 2002).
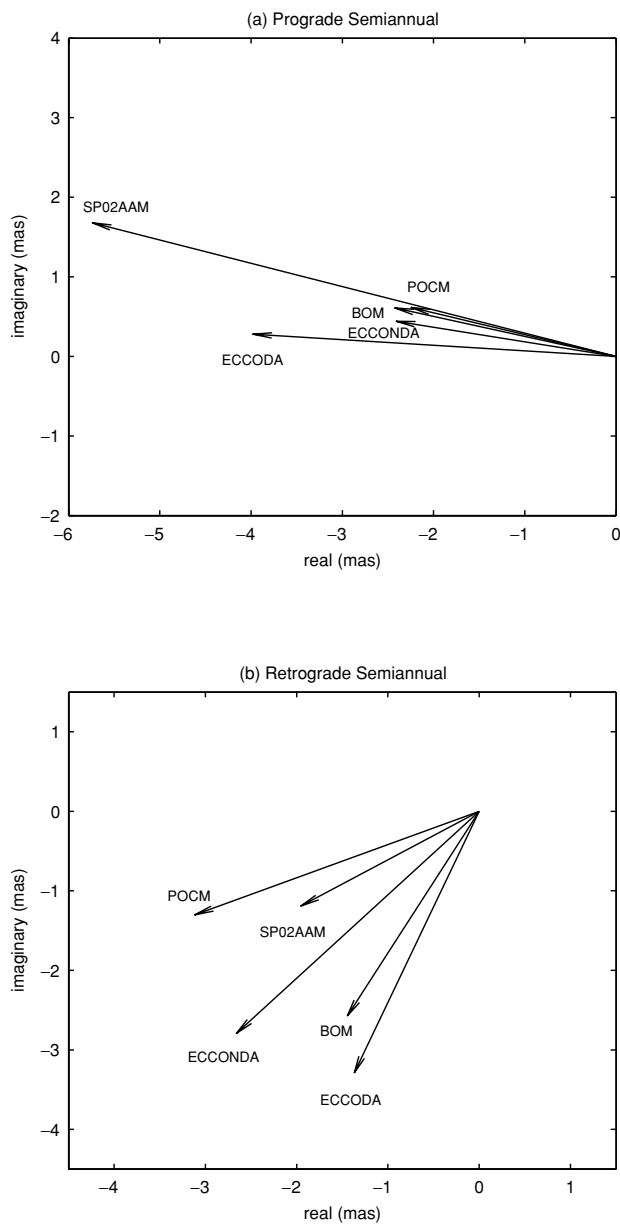
Figure 5. As in Fig. 2 but for the semi-annual polar motion excitations.

Figure 6. As in Fig. 2 but for the terannual polar motion excitations.

(2) The oceanic movements at short periods are characteristic of barotropic motion, which is more effective than baroclinic motion in transporting mass laterally (Wahr *et al.* 1998).

5 SUMMARY

In this study, we analyse and compare observed non-atmospheric polar motion excitations with OAM variations determined from four OGCMs: the POCM, BOM, ECCO-NDA and ECCO-DA, during a 5-yr overlapped period from 1993 to 1997. At annual timescale, none of the four OAM estimates agree well with observed excitations. Since hydrological effects, which are believed to be significant at seasonal timescales, are not considered here, the comparison (at seasonal timescales) is focused on internal agreement among the four ocean models. Considerable discrepancies exist between POCM and the other three models, which are mainly due to differences in the forcing wind fields. At semi-annual timescale, however, POCM has
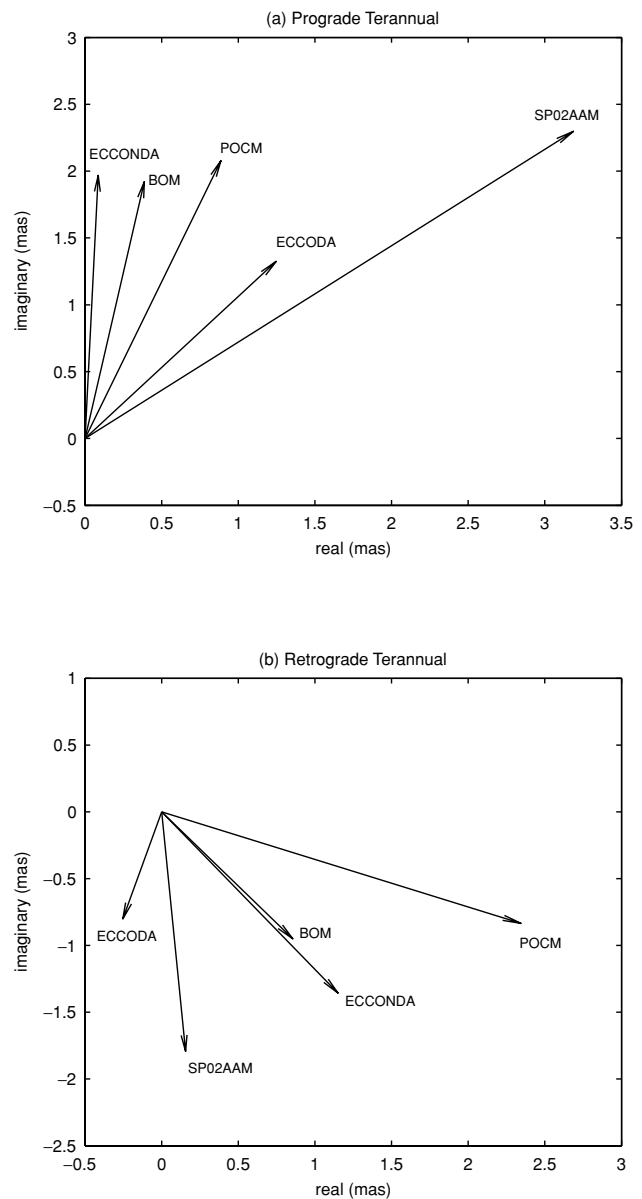
generally better agreement with observed non-atmospheric polar motion excitation than the other three ocean models.

At intraseasonal timescales, ECCO-DA yields better agreement with observations, and reduces the variance of non-atmospheric excitations by ∼60, 10–20 per cent more than those explained by the other three models. However, at the very short periods of 4–20 days, the BOM estimates could explain about half of the observed variance, twice as much as that by ECCO-NDA, and also shows considerably better correlation with observations. The superiority of BOM to ECCO-NDA in modelling very high-frequency OAM variations might indicate the characteristically barotropic oceanic motion at short periods and the importance of including pressure-forcing effects when modelling the high-frequency variability of the ocean.

The considerable discrepancies among four OGCMs in the estimation of oceanic excitations to the Earth's polar motion might be owing to differences in modelling schemes and methods, ambiguity between barotropic and baroclinic effects, the Bossinesq

Table 4. Cross correlation coefficients between intraseasonal SPACE2002-AAM and oceanic effects modelled from the four OGCMs, and variance reductions (in percentage) when the oceanic excitations are removed from SPACE2002-AAM. (A) OBP terms; (B) Currents terms; (C) OBP plus Currents terms.

Excitation function	X		Y		X + iY	
	Corr. coef.	Reduced var. (per cent)	Corr. coef.	Reduced var. (per cent)	Corr. coef.	Reduced var. (per cent)
(A) OBP						
POCM	0.42	17.0	0.65	38.8	0.59	33.2
BOM	0.54	28.8	0.60	28.2	0.57	28.3
ECCO-NDA	0.61	35.8	0.63	34.6	0.62	34.9
ECCO-DA	0.66	41.9	0.74	47.8	0.72	46.3
(B) Currents						
POCM	0.47	22.5	0.62	28.5	0.56	27.0
BOM	0.55	28.0	0.54	18.6	0.53	21.0
ECCO-NDA	0.54	27.2	0.60	21.8	0.56	23.2
ECCO-DA	0.53	26.8	0.70	25.6	0.60	25.9
(C) OBP+Currents						
POCM	0.63	39.6	0.69	47.3	0.67	45.3
BOM	0.67	45.0	0.65	39.0	0.65	40.5
ECCO-NDA	0.74	54.7	0.69	45.9	0.70	48.2
ECCO-DA	0.78	61.3	0.80	60.7	0.79	60.9

X: x component; Y: y component; Corr. coef.: correlation coefficient; Reduced var.: reduced variance.
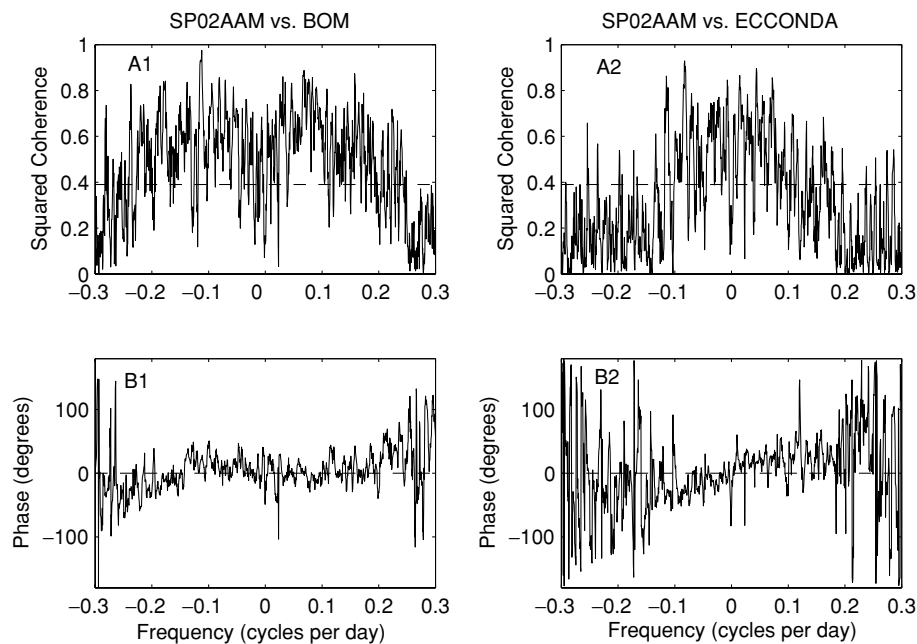

Figure 7. (A1, A2) multitaper squared coherences and (B1, B2) phases of the SPACE2002-AAM with oceanic excitations modelled from the BOM and ECCO-NDA. A trend, annual, semi-annual and terannual variations have been removed from all time-series by least-squares fitting. The horizontal dash lines in A1 and A2 indicate 95 per cent confidence threshold for the squared coherence.

approximation conserving ocean volume rather than conserving mass and non-global coverage of OGCMs (Greatbatch 1994; Wahr *et al.* 1998). Mass-conserving OGCMs (e.g. Huang *et al.* 2001) that assimilates altimeter sea level, sea surface temperature, and salinity data and is driven by winds, fluxes, and also atmospheric pressure that are being developed may be useful in a better understanding of the effects of these model differences. In the longer term, fully coupled models that conserve mass within the full atmosphere–ocean–hydrosphere system are needed. Assimilation of satellite gravity observations, such as those from the Gravity Recovery and Climate Experiment mission (http://www.csr.utexas.edu/grace/), could lead to important improvement in OGCM development, as well.

Table 5. As in Table 4 but for high-frequency variations of 4–20 days. The POCM and ECCO-DA are not included because their relatively large sampling intervals obstruct analyses of the high-frequency variations.

Excitation function	*X*		*Y*		*X* + *iY*	
	Corr. coef.	Reduced var. (per cent)	Corr. coef.	Reduced var. (per cent)	Corr. coef.	Reduced var. (per cent)
(A) OBP						
BOM	0.66	42.6	0.67	42.8	0.67	42.8
ECCO-NDA	0.55	22.6	0.50	22.1	0.51	22.3
(B) Currents						
BOM	0.33	7.3	0.58	30.6	0.52	22.0
ECCO-NDA	0.22	−2.2	0.33	10.7	0.28	5.9
(C) OBP+Currents						
BOM	0.71	49.5	0.73	52.9	0.73	51.6
ECCO-NDA	0.57	26.2	0.52	24.0	0.54	24.8

REFERENCES

Chao, B.F. & Au, A.Y., 1991. Atmospheric excitation of the Earth's annual wobble: 1980–1988, *J. geophys. Res.,* **96,** 6577–6582.

Chao, B.F. & O'Connor, W.P., 1988. Effect of a uniform sea-level change on the Earth's rotation and gravitational field, *Geophys. J. R. astr. Soc.,* **93,** 191–193.

Chen, J.L., Wilson, C.R., Chao, B.F., Shum, C.K. & Tapley, B.D., 2000. Hydrologic and oceanic excitations to polar motion and length-of-day variation, *Geophys. J. Int.,* **141,** 149–156.

Chen, J.L., Wilson, C.R., Hu, X.G., Zhou, Y.H. & Tapley, B.D., 2004. Oceanic effects on polar motion determined from an ocean model and satellite altimetry: 1993–2001, *J. geophys. Res.,* **109**(B2), B02411, doi:10.1029/2003JB002664.

Eubanks, T.M., 1993. Variations in the orientation of the Earth, in *Contributions of space geodesy to geodynamics: Earth dynamics, Geodyn. Ser.,* Vol. 24, pp. 1–54, eds Smith, D.E. & Turcotte, D.L., AGU, Washington, DC.

Greatbatch, R.J., 1994. A note on the representation of steric sea level in models that conserve volume rather than mass, *J. geophys. Res.,* **99,** 12 767–12 771.

Gross, R.S., 2003a. Combinations of Earth orientation measurements: SPACE2002, COMB2002, and POLE2002, *JPL Publ.,* **03–11,** 28.

Gross, R.S., Fukumori, I. & Menemenlis, D., 2003b. Atmospheric and oceanic excitation of the Earth's wobbles during 1980–2000, *J. geophys. Res.,* **108**(B8), 2370, doi:10.1029/2002JB002143.

Huang, R.X., Jin, X.Z. & Zhang X.H., 2001. An ocean general circulation model in pressure coordinates, *Advances in Atmospheric Science,* **18,** 1–22.

Johnson, T.J., 2005. The interannual spectrum of the atmosphere and oceans, Proceedings of the Chandler Wobble Workshop 2004, European Center for Geodynamics and Seismology, Luxembourg.

Johnson, T.J., Wilson, C.R. & Chao, B.F., 1999. Oceanic angular momentum variability estimated from the Parallel Ocean Climate Model, 1988–1998, *J. geophys. Res.,* **104,** 25 183–25 195.

Kalnay, E. *et al.*, 1996. The NCEP/NCAR 40-yr reanalysis project, *Bulletin of the American Meteorological Society,* **77,** 437–471.

Kuehne, J. & Wilson, C.R., 1991. Terrestrial Water Storage and Polar Motion, *J. geophys. Res.,* **96,** 4337–4345.

Lambeck, K., 1980. *The Earth's variable rotation*, Cambridge University Press, New York.

Marshall, J., Hill, C., Perelman, L. & Adcroft, A., 1997a. Hydrostatic, quasi-hydrostatic, and nonhydrostatic ocean modelling, *J. geophys. Res.,* **102,** 5733–5752.

Marshall, J., Adcroft, A., Hill, C., Perelman, L. & Heisey, C., 1997b. A finite-volume, incompressible, Navier Stokes model for studies of the ocean on parallel computers, *J. geophys. Res.,* **102,** 5753–5766.

Munk, W.H. & MacDonald, G.J.F., 1960. *The rotation of the Earth: a geophysical discussion*, Cambridge University Press, New York.

Nastula, J., Ponte, R.M. & Salstein, D.A., 2002. Regional high-frequency signals in atmospheric and oceanic excitation of polar motion, *Adv. Space. Res.,* **30,** 369–374.

Ponte, R.M., 1993. Variability in a homogeneous global ocean forced by barometric pressure, *Dynamics of Atmosphere and Oceans,* **18,** 209–234.

Ponte, R.M. & Ali, A.H., 2002. Rapid ocean signals in polar motion and length of day, *Geophys. Res. Lett.,* **29,** 61–64.

Ponte, R.M. & Stammer, D., 1999. Role of ocean currents and bottom pressure variability on seasonal polar motion, *J. geophys. Res.,* **104,** 23 393–23 410.

Ponte, R.M., Stammer, D. & Marshall, J., 1998. Oceanic signals in observed motions of the Earth's pole of rotation, *Nature,* **391,** 476–479.

Ponte, R.M., Stammer, D. & Wunsch, C., 2001. Improving ocean angular momentum estimates using a model constrained by data, *Geophys. Res. Lett.,* **28,** 1775–1778.

Salstein, D.A., Kann, D.M., Miller, A.J. & Rosen, R.D., 1993. The sub-bureau for atmospheric angular momentum of the interannual earth rotation service: a meteorological data center with geodetic applications, *Bull. Am. Meteor. Soc.,* **74,** 67–80.

Stammer, D., Tokmakian, R., Semtner, A. & Wunsch, C., 1996. How well does a 1/4° global circulation model simulate large-scale ocean observations? *J. geophys. Res.,* **101,** 25 779–25 812.

Stammer, D., Wunsch, C., Fukumori, I. & Marshall, J., 2002. State estimation improves prospects for ocean research, *EOS Trans.,* **83,** 289–295.

Thomson, D.J., 1982. Spectrum estimation and harmonic analysis, *IEEE. Proc.,* **70,** 1055–1096.

Wahr, J., 1982. The effects of the atmosphere and oceans on the Earth's wobble: I. Theory, *Geophys. J. R. astr. Soc.,* **70,** 349–372.

Wahr, J., 1983. The effects of the atmosphere and oceans on the Earth's wobble and on the seasonal variations in the length of day: II. Results, *Geophys. J. R. astr. Soc.,* **74,** 451–487.

Wahr, J., Molenaar, M. & Bryan, F., 1998. Time variability of the Earth's gravity field: hydrological and oceanic effects and their possible detection using GRACE, *J. geophys. Res.,* **103,** 30 205–30 229.

Wiley, J., 1979. *Programs for digital signal processing*, IEEE Press, New York

Wilson, C.R., 1985. Discrete polar motion equations, *Geophys. J. R. astr. Soc.,* **80,** 551–554.

Wilson, C.R. & Chen, J.L., 1996. Discrete polar motion equations for high frequencies, *J. Geodyn.,* **70,** 581–585.

Wilson, C.R. & Vicente, R.O., 1990. Maximum likelihood estimates of polar motion parameters, in *Variations in Earth Rotation*, pp. 151–155, eds McCarthy, D.D., Carter, W.E., *Am. Geophys. Un. Geophys Monogr. Series*, Washington, DC.

Zhou, Y.H., Zheng, D.W., Zhao, M. & Chao, B.F., 1998. Interannual polar motion with relation to the North Atlantic Oscillation, *Global and Planet Change,* **18,** 79–84.